Available online at www.sciencedirect.com
ScienceDirect
Infrared Physics & Technology 50 (2007) 191–193
INFRARED PHYSICS & TECHNOLOGY
www.elsevier.com/locate/infrared

Design of terahertz quantum well photodetectors

H.C. Liu [a,*], H. Luo [a], C.Y. Song [a], Z.R. Wasilewski [a], A.J. Spring Thorpe [a], J.C. Cao [b]

[a] Institute for Microstructural Sciences, National Research Council, Ottawa, Canada K1A 0R6
[b] State Key Laboratory of Functional Materials for Informatics, Shanghai Institute of Microsystem and Information Technology, Chinese Academy of Sciences, Shanghai 200050, China

Available online 17 November 2006

Abstract

Design considerations of terahertz quantum well photodetectors are presented. Quantum well parameters are determined by the condition of having the first excited state in resonance with the top of the barrier. Due to the small transition energy many body effects need to be included to accurately predict the spectral response peak position. A trade-off in doping density between absorption strength and operating temperature needs to be made. Predictions are compared with experiments and future directions are pointed out.

1. Introduction

For the thermal infrared region of wavelengths 3–14 μm, the quantum well infrared photodetector (QWIP) is becoming a true technology [1–3]. For a standard GaAs/AlGaAs QWIP the materials parameters and design considerations are well established [2,3]. For the terahertz (THz) region (frequency 1–10 THz or wavelength 30–300 μm), however, only limited investigations have been carried out [4–6]. Here we present design considerations for THz QWIPs and compare modeling with experiments. We discuss the quantum well parameters, barrier thickness, doping density, and their resulting performance characteristics such as absorption, and background limited infrared performance (BLIP) temperature. In our previous work, [4,5], many body effects were neglected. We show here that these effects need to be included to accurately predict the response wavelength.

2. Design and analysis

We consider only THz QWIPs made of the GaAs/AlGaAs materials system and grown by molecular beam epitaxy (MBE). Not fully tested, but expected to be valid, at least as a good approximation, the conduction band offset or the barrier height is given by $V_b = 0.87 \times x$ (eV), where x is the Al fraction. The optimum QW parameter for a standard QWIP is to have the first excited state in resonance with the top of the barrier [2,3]. With this condition and neglecting the many body effects on the first excited state, the well width and the barrier aluminium percentage are easily calculated for a simple square quantum well (Fig. 1).

Neglecting the many body effects, the range of parameters in Fig. 1 would result in a detection peak frequency in the range of about 0.8–8 THz [4], however, this was in disagreement with experiments [5]. Although the doping densities used in THz QWIPs are low and many body corrections are small, the THz photon energies are also small and therefore the corrections need to be included. The many body effects include exchange-correlation and depolarization [3]. As these corrections depend on doping density, we need to choose the doping for a given quantum well. To have the highest possible dark current limited detectivity D^*, the doping density n_{2D} in the well is determined using the established relations [2,3]: $E_f = 2k_B T$ and $n_{2D} = (m^*/\pi\hbar^2)E_f$, where E_f is the Fermi energy, and m^* is the effective mass in the well. This requires choosing the operating temperature T. Commonly in practice, given

* Corresponding author. Tel.: +1 613 993 3895; fax: +1 613 990 0202.
E-mail address: h.c.liu@nrc.ca (H.C. Liu).

1350-4495/$ - see front matter © 2006 Elsevier B.V. All rights reserved.
doi:10.1016/j.infrared.2006.10.026

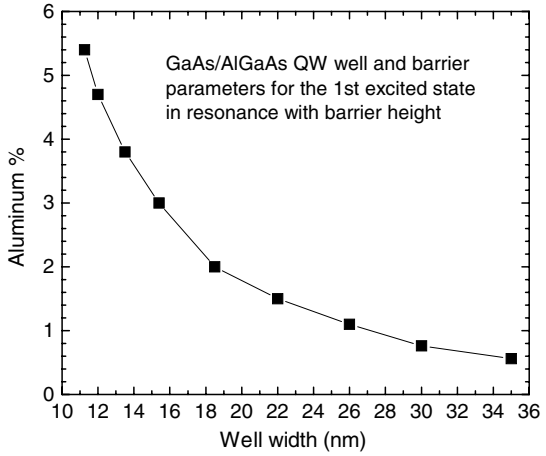

Fig. 1. Calculated quantum well (QW) parameters.

a detection photon energy hv, the operating temperature often corresponds k_BT many times less than hv, for example $k_BT \sim hv/20$. For the THz regime, one then would expect the operating temperature around 20 K and below. However, if sufficient cooling is available for operation under BLIP condition, the doping may be increased to enhance the absorption. The doping densities used for the following test devices correspond to BLIP operating temperature in the range from 10 K to 20 K.

Having determined the quantum well and doping parameters, the next design parameter is the barrier width. The barrier width should be sufficiently thick so that the dark current is completely in the thermionic regime, i.e., inter-well tunneling should be negligible comparing to the background photocurrent. The background photocurrent for a usual environment (~300 K) is no more than 10^{-5} A/cm^2. The inter-well tunneling current can be easily estimated [3], and the results for three barrier x values are shown in Fig. 2. The estimate used the doping densities in the following test devices. One may then choose the barrier widths $L_b = 55$, 70, and 95 nm for $x = 0.05$, 0.03, and 0.015 QWIPs, respectively.

3. Experimental

Three wafers were grown by MBE on semi-insulating GaAs substrates and devices were made by standard GaAs microfabrication methods. The MBE layers consist of (starting from the substrate) a 800-nm GaAs bottom contact doped with Si to 10^{17} cm^{-3}, N QWs with L_w thick GaAs wells and L_b thick AlGaAs barriers, and a 400-nm GaAs top contact doped with Si to 10^{17} cm^{-3}. Each GaAs well center 10-nm region was doped with Si to N_d. Other parameters are given in Table 1. Square mesa devices with various sizes were tested and their characteristics scaled appropriately, indicating an excellent uniformity. One facet of each device chip was polished to an angle of 45° for coupling of the light into the quantum wells. Another piece from each wafer was polished with two parallel 45° facets for transmission measurement to assess the strength of the absorption. The length of these zigzag waveguides was chosen to give two double passes for the infrared beam, i.e., four times the wafer thickness. As reported before [5], these devices do reach BLIP at temperatures of 17, 13, and 12 K, respectively, and their responsivity values are comparable to standard thermal infrared QWIPs. Absorption measurements were attempted on all zigzag waveguides, however, due to the phonon absorption, only V267 yielded meaningful results (Fig. 3), which are consistent with calculations [2,3]. The absorption strength is low for these test devices due to the low doping and the relatively small number of wells used. These are being improved in our on-going iteration.

Table 1
Wafer parameters

Wafer	L_w (nm)	L_b (nm)	N	[Al] (%)	N_d (cm^{-3})	n_{2D} (cm^{-2})
V265	11.9	55.2	40	5	1E17	1E11
V266	15.5	70.2	30	3	6E16	6E10
V267	22.1	95.1	23	1.5	3E16	3E10

The Si doping N_d is over the center 10 nm of the GaAs well, resulting in a two-dimensional electron density of n_{2D}.

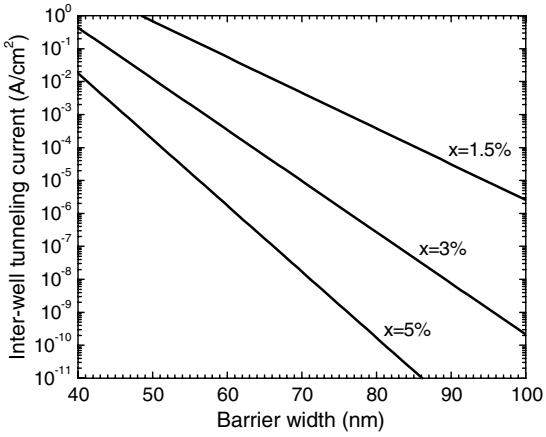

Fig. 2. Estimated inter-well tunneling current.

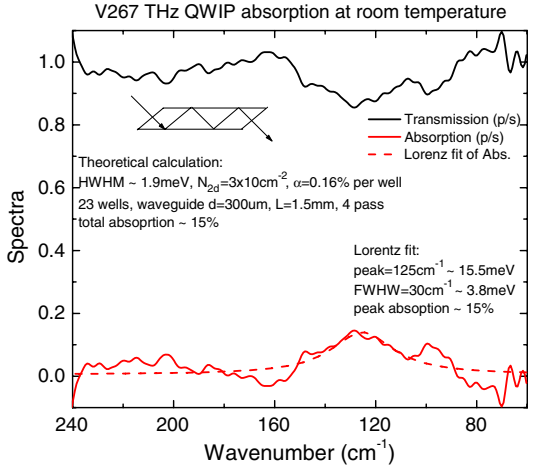

Fig. 3. Polarized transmission and absorption spectra.

The experimental spectral response curves for all three samples are shown in Fig. 4. As the spectrum for V265 overlaps with the phonon absorption region, the true peak is difficult to determine, and is estimated to be about 290 cm^{-1} (36 meV). For the other two samples, the peaks are determined to be at 180 (22.3) and 108 cm^{-1}(13.4 meV), respectively.

Simple calculations without including many body effects lead to results in disagreement with experiments. For example, $E_2 - E_1$ in Table 2 for sample V267 differs from experiment by about 40%. We consider both static and dynamic many body effects, namely exchange-correlation and depolarization [2,3]. We tried both the expression given by Bandara et al. [7] (which includes only exchange) and the expression for an ideal two-dimensional electron gas [8]. It is found that the latter gives better agreement with experiments, which is used for Table 2. This is perhaps due to the low doping regime for THz QWIPs and the Bandara's formula includes only exchange, more applicable to high density. For the depolarization effect, we use the formula given in Ref. [9]. Comparing the last two columns in Table 2, obviously the expected peak response energy is now in reasonable agreement with experiments.

We also compared measured activation energy with theory. The activation energy corresponding to the energy from the top of the Fermi sea to the top of the barrier can be deduced from the results of current–voltage characteristics at various temperatures. The values for zero bias for the three devices are 28.2, 17.1, and 8.6 meV, respectively. Theoretically the activation energy is $V_b - E_1 + E_{ex\text{-}co} - E_f = 30.30$, 19.07, and 10.20 meV for the three samples, respectively. In this case, the theoretical values are all slightly larger than those for experiments, though not very large. Note that the activation energy is measured from the dark current and it reflects how well the barrier behaves versus ideal expectations. There may be extra leakage current due to the very low Al fractions used in these devices, and perhaps the random alloy in this very low Al regime results in a non-uniform barrier. This issue should be investigated further.

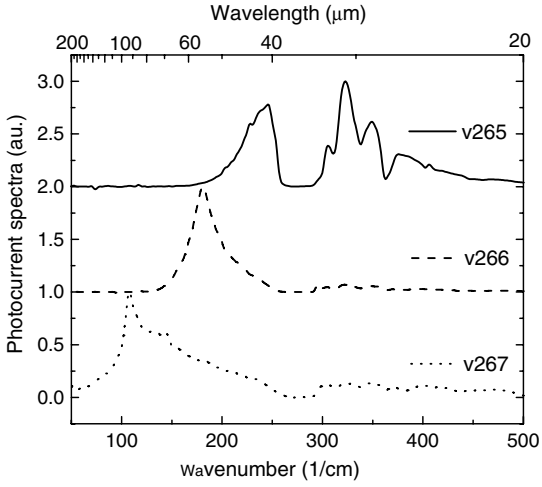

Fig. 4. Photocurrent spectral response spectra at 8 K.

Table 2
Comparison of expected and measured response peak energies

Wafer	n_{2D} (cm^{-2})	E_1 (meV)	E_2 (meV)	$E_{ex\text{-}co}$ (meV)	E_{depol} (meV)	Theory peak (meV)	Exp peak (meV)
V265	1E11	14.31	43.21	4.71	2.2	35.81	~36
V266	6E10	8.58	26.93	3.65	1.6	23.60	22.3
V267	3E10	4.25	12.92	2.50	1.0	12.17	13.4

The symbols are E_1 – ground state energy, E_2 – first excited state energy, $E_{ex\text{-}co}$ – exchange-correlation energy, and E_{depol} – depolarization energy. The expected theoretical spectral peak position is given by $E_2 - E_1 + E_{ex\text{-}co} + E_{depol}$. Note that E_2 is very close to the barrier height.

4. Conclusion

We have presented the design considerations for THz QWIPs and compared experimental results with model calculations. It is established that for THz QWIPs many body effects must be included. The next improvement needed is the absorption, by both increasing the doping and the number of wells. Future directions include developing imaging devices and testing the high speed characteristics for THz communication and heterodyne applications.

Acknowledgements

This work was supported in part by the NRC GHI program and by the National Fund for Distinguished Young Scholars of China (60425415 and 60528005).

References

[1] S.D. Gunapala, S.V. Bandara, in: H.C. Liu, F. Capasso (Eds.), Intersubband Transition in Quantum Wells: Physics and Device Applications I, Semiconductors and Semimetals, vol. 62, Academic, San Diego, 2000, pp. 197–282 (Chapter 4).
[2] H.C. Liu, in: H.C. Liu, F. Capasso (Eds.), Intersubband Transition in Quantum Wells: Physics and Device Applications I, Semiconductors and Semimetals, vol. 62, Academic, San Diego, 2000, pp. 126–196 (Chapter 3).
[3] H. Schneider, H.C. Liu, Quantum Well Infrared Photodetectors: Physics and Applications, Springer, Berlin, 2006.
[4] H.C. Liu, C.Y. Song, A.J. Spring Thorpe, J.C. Cao, Appl. Phys. Lett. 84 (2004) 4068.
[5] H. Luo, H.C. Liu, C.Y. Song, Z.R. Wasilewski, Appl. Phys. Lett. 86 (2005) 231103.
[6] M. Graf, G. Scalari, D. Hofstetter, J. Faist, H. Beere, E. Linfield, D. Ritchie, G. Davies, Appl. Phys. Lett. 84 (2004) 475.
[7] K.M.S.V. Bandara, D.D. Coon, O. Byungsung, Y.F. Lin, M.H. Francombe, Appl. Phys. Lett. 53 (1988) 1931;
K.M.S.V. Bandara, D.D. Coon, O. Byungsung, Y.F. Lin, M.H. Francombe, Appl. Phys. Lett. 55 (1989) 206.
[8] A. Ishihara, in: H. Ehrenreich, D. Turnbull (Eds.), Solid State Physics, vol. 42, Academic, Boston, 1989, p. 271.
[9] W.P. Chen, Y.J. Chen, E. Burstein, Surf. Sci. 58 (1976) 263.